Journal of Southeast University (English Edition) Vol. 27, No. 3, pp. 253 – 256 Sept. 2011 ISSN 1003—7985

Effect of viscoelasticity on nonlinear vibration of single microbubble

Yang Li Yang Fang Chen Ping Gu Ning

(State Key Laboratory of Bioelectronics, Southeast University, Nanjing 210096, China)
(Jiangsu Key Laboratory for Biomaterials and Devices, Southeast University, Nanjing 210096, China)

Abstract: Based on the Church-Hoff model, the nonlinear oscillations of a single encapsulated microbubble with a finite thickness shell are theoretically studied. The effects of viscoelasticity on radial oscillations and the fundamental and harmonic components are researched. The peaks of radial oscillations and magnitudes of power spectra of the fundamental and harmonic components all increase gradually with the shear modulus of shell varying from 0 to 10 MPa by an interval of 0.1 MPa at the same shear viscosity, while they decrease as the shear viscosity increases from 0 to 1 Pa · s by an interval of 0.01 Pa · s at the same shear modulus. The fluctuation ranges of subharmonic and ultraharmonic signals are much larger than both the fundamental and second harmonic components. It means that the effect of viscoelasticity on the subharmonic and ultraharmonic signals is greater than that on the fundamental and second harmonic components. So adjusting the viscoelasticity of the shell is a potential method to obtain a perfect microbubble contrast agent used for the subharmonic and ultraharmonic imaging. Four points with significant fundamental and harmonic components are chosen as an example: a shear viscosity of 0.39 Pa · s with shear modulus of 3.9, 6.6, and 8.6 MPa, respectively; a shear modulus of 6.6 MPa with a shear viscosity of 0.42 Pa · s.

Key words: microbubble; viscoelasticity; radial oscillation; harmonic imaging
doi: 10.3969/j.issn.1003 – 7985.2011.03.005

Commercially available ultrasound contrast agents (UCA) are usually microbubbles of 1 to 10 μm in diameter, consisting of lipid, protein, or polymer shells[1] and are usually filled with inert-gas. Since the UCA can effectively enhance the backscattering signal intensity, they have received wide attention. When insonated by ultrasound (US) of frequency f_0, due to their nonlinear vibrational nature, UCA microbubbles can not only return echo signals with the same frequency but also send back signals with subharmonics $f_0/2$[2], harmonics ($2f_0$, $3f_0$, $4f_0$, …) and ultraharmonics ($3f_0/2$, $5f_0/2$, $7f_0/2$)[3-6]. Subharmonic signals are expected to provide a higher contrast between biological tissues and blood flow because the echo signals are generated only from blood containing the contrast agents. Hence, subharmonic or ultraharmonic imaging should have advantages as an US imaging technique[7-8]. One disadvantage of subharmonic imaging is that echo signals are usually weak. So the enhancement of echo signals becomes an urgent task to make subharmonic imaging effective in clinical applications.

Viscoelasticity of the shell plays an important role in the nonlinear vibration of the coated microbubble[9]. The viscoelasticity of different shell materials may be different. In experiment, the viscoelasticity of ultrasound contrast agents can be changed by selecting different shell materials or modifying the shell with various targeted antibodies or nanoparticles[10-11]. In this paper, we try to optimize the backscattering signals by adjusting the viscoelasticity through numerical analysis. Our goal is to give some theoretical guidance for producing microbubbles of UCA which can generate rich subharmonic echo components for better imaging.

1 Theoretical Background

The theoretical description of the nonlinear oscillations under US excitation for a UCA microbubble is based on the Hoff model[12]. The UCA microbubble considered here is an air bubble enclosed in a solid, incompressible viscoelastic shell (see Fig. 1). The shell is described by shear modulus G_s and shear viscosity μ_s. The surrounding medium is blood-like and modeled as a Newtonian fluid with shear viscosity. The shear modulus G_s and shear viscosity μ_s of a polymeric material are in general frequency dependent. The sound beam with a frequency of 2.25 MHz, one of the commonly used frequencies in diagnostic medical imaging, is used to insonate the microbubble. The equation is further assumed that the existence of the shell reduces surface tensions at the shell-liquid and shell-gas interfaces, so that surface tension can be ignored and there is no tension in the shell at equilibrium.

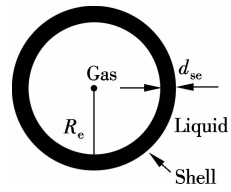

Fig. 1 Schematic diagram of an encapsulated air-filled microbubble

The Hoff equation can be written as

$$\rho_l\left(\ddot{R}R+\frac{3}{2}\dot{R}^2\right)=P_0\left(\left(\frac{R_e}{R}\right)^{3k}-1\right)-P_a(t)-4\mu_l\frac{\dot{R}}{R}-12\mu_s\frac{d_{se}R_e^2\dot{R}}{R^4}-12G_s\frac{d_{se}R_e^2}{R^3}\left(1-\frac{R_e}{R}\right) \quad (1)$$

where R is the instantaneous radius of the bubble; $\dot{R}$, $\ddot{R}$ are the first and the second time derivatives of the instantaneous radius, respectively; R_e is the equilibrium radius; P_0 is the ambient pressure; d_{se} is the shell thickness at rest; μ_l is the

Received 2011-03-31.
Biographies: Yang Li (1986—), female, graduate; Gu Ning (corresponding author), male, doctor, professor, guning@seu.edu.cn.
Foundation items: The National Basic Research Program of China (973 Program) (No. 2011CB933503), the National Natural Science Foundation of China (No. 50872021, 60725101, 31000453).
Citation: Yang Li, Yang Fang, Chen Ping, et al. Effect of viscoelasticity on nonlinear vibration of single microbubble[J]. Journal of Southeast University (English Edition), 2011, 27(3): 253 – 256. [doi: 10.3969/j.issn.1003 – 7985.2011.03.005]

shear viscosity in the surrounding medium; G_s is the shear modulus of the shell and μ_s is shear viscosity of the shell. $P_a(t)$ is the time-varying incident acoustic pressure.

Using a prepared Matlab code implementing a fourth-order Runge-Kutta procedure (Matlab function ODE45), Eq. (1) is solved numerically for the following set of parameters: $R_e = 5$ μm; $d_{se} = 0.05R_e$; $\mu_l = 0.001$ Pa · s; $P_0 = 101.3$ kPa; $P_a(t) = A\sin(2\pi f_c t)$; $A = 480$ kPa and $f_c = 2.25$ MHz. In all of the simulations, the initial conditions are $R(0) = R_e$, $\dot{R}(0) = 0$ and $\ddot{R}(0) = 0$.

2 Results

2.1 Effects of viscoelasticity of shell on radial oscillations

We are now set to examine the parameter space for the unknown parameters, instantaneous radius $R(t)$ and shear viscosity μ_s, using the driving pressure of 480 kPa for an initial bubble size of $R_e = 5$ μm and $P_a(t) = A\sin[(2\pi \times 2.25 \times 10^6 t)]$.

First of all, the changes of radius $R(t)$ are studied with different shear viscosities of shell. Varying shear viscosities from 0.1 to 0.39 Pa · s and then to 1 Pa · s at the same shear modulus of 6.6 MPa, the effect of shear viscosity on the oscillation radius can be worked out. Fig. 2(a) shows that the magnitudes of the negative resonance peak of standardized microbubble oscillation radius at the shear viscosity of 0.1,

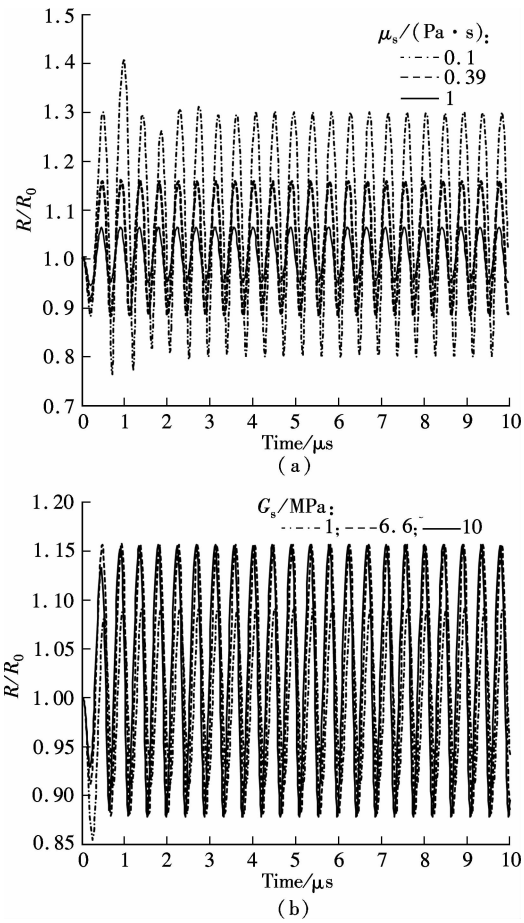

Fig. 2 Oscillation radius $R(t)$ changing with different viscoelasticities. (a) With the shear viscosity of 0.1, 0.39 and 1 Pa · s at shear modulus of 6.6 MPa; (b) With the shear modulus of 1, 6.6 and 10 MPa at shear viscosity of 0.39 Pa · s

0.39 and 1 Pa · s are about 0.80, 0.88 and 0.95, respectively.

Using a similar method, the effect of shear modulus on the microbubble oscillation is investigated. Changing the shear modulus from 1 to 6.6 MPa and then to 10 MPa at the same shear viscosity of 0.39 Pa · s, the effect of shear modulus on the oscillation radius can be studied. Fig. 2(b) shows that the magnitudes of the negative peak of the standardized microbubble oscillation radius at the shear modulus of 1, 6.6 and 10 MPa are about 0.91, 0.88 and 0.87, respectively.

From the above analysis, the effect of the shear viscosity and the shear modulus on microbubble oscillations is easy to understand. The shear viscosity, to a certain extent, prevents the microbubble oscillations because the shear modulus is the stiffness parameter, while the shear modulus as a rigid parameter can enhance the microbubble oscillations. Hence, the expected radial oscillations of the encapsulated microbubble can be obtained by adjusting the viscoelasticity of the microbubble moderately.

2.2 Effect of shell viscoelasticity on nonlinear oscillations

Eq. (1) is solved using the fourth-order Runge-Kutta algorithm. The pressure $P_s(t)$ scattered by an encapsulated microbubble at a distance r from the center of the bubble can be expressed as[13]

$$P_s(t) = \rho_l \frac{R}{r}(2\dot{R}^2 + R\ddot{R}) \tag{2}$$

2.2.1 Effect of shell shear viscosity

We are now set to examine the effects of shear viscosity on microbubble nonlinear oscillations by changing the shear viscosity from 0 to 1 Pa · s by an interval of 0.01 Pa · s at the same shear modulus of 6.6 MPa.

As can be seen in Fig. 3(a), with the increase in viscosity, the fundamental, subharmonic, ultraharmonic and second harmonic contents gradually decrease. The amplitudes of the fundamental and the second harmonic components fluctuate around −12.27 and −24.50 dB, respectively. Moreover, the amplitudes of the subharmonic and ultraharmonic components fluctuate around −38.55 dB. The curve of the subharmonic component has some large positive peaks such as at 0.39 and 0.42 Pa · s, and their amplitudes are −31.20 and −34.59 dB, respectively. The curve of the ultraharmonic component also has large positive peaks at these two points, and their amplitudes are −29.97 and −32.29 dB, respectively.

2.2.2 Effect of shell shear modulus

Then the impact of the shear modulus on nonlinear oscillations can be investigated by comparing the fundamental and harmonics components at varied shear moduli under the shear viscosity of 0.39 Pa · s.

Fig. 3(b) shows four curves, which represent the fundamental, second harmonic, subharmonic and ultraharmonic components, respectively. Changing the shear modulus from 0 to 10 MPa by an interval of 0.1 MPa at the same shear viscosity of 0.39 Pa · s, the effects of shear viscosity on the fundamental and harmonic components can be obtained. This figure also presents that the curves increase slowly with the increase in the shear modulus. The amplitudes of the fundamental and the second harmonic compo-

nents fluctuate around −11.28 dB and −24.85 dB, respectively. In addition, the subharmonic and ultraharmonic components vary around −37.96 dB. The curve of the subharmonic component has some large positive peaks such as at 3.9, 6.6 and 8.6 MPa, and their amplitudes are −32.55, −31.20 and −39.67 dB, respectively. The curve of the ultraharmonic component also has three large positive peaks at these three points, and their amplitudes are −36.45, −29.97 and −33.92 dB, respectively.

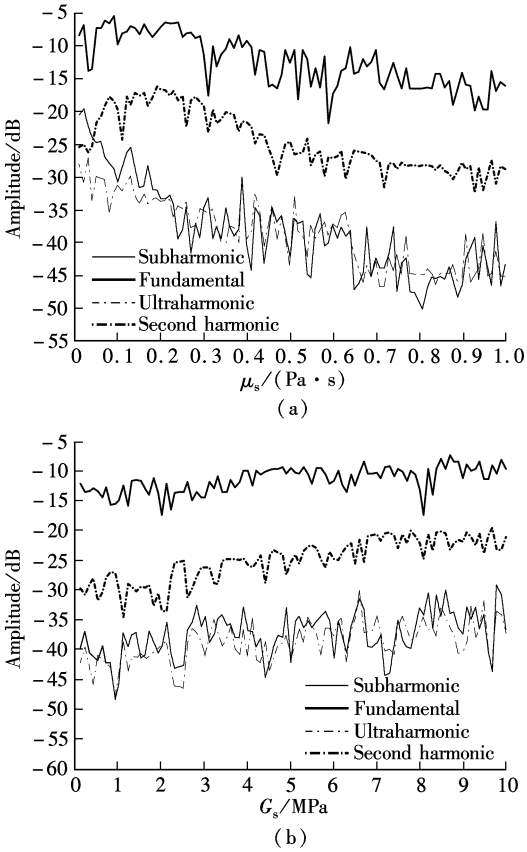

Fig. 3 The fundamental and harmonic components varying with shear modulus and shear viscosity. (a) At shear modulus of 6.6 MPa; (b) At shear viscosity of 0.39 Pa · s

2.2.3 Significant fundamental and harmonic components

According to the above analysis, considering the consequences of the fundamental and harmonic imaging, the power spectrums of backscattered pressure from microbubbles at four points, the shear viscosity of 0.39 and 0.42 Pa · s with a shear modulus of 6.6 MPa, and the shear moduli of 3.9 and 8.6 MPa with a shear viscosity of 0.39 are worked out.

From Fig. 4, it can be seen that the fundamental, second harmonic, subharmonic and ultraharmonic components are all very significant. In Fig. 4(a), the amplitudes of the fundamental, second, subharmonic and ultraharmonic components are −10.24, −24.51, −32.55 and −36.45 dB, respectively.

In Fig. 4(b), the amplitudes of the fundamental, second, subharmonic and ultraharmonic components are −10.05, −21.36, −31.20 and −29.97 dB, respectively. In addition, 3f, 4f, 5f/2 and 7f/2 harmonic components are also extraordinary. So the conclusion can be drawn: the shell with a shear modulus of 6.6 MPa and a shear viscosity of 0.39 Pa · s is fit for both fundamental and harmonic imaging, especially for the subharmonic imaging.

In Fig. 4(c), the amplitudes of the fundamental, second, subharmonic and ultraharmonic components are −9.80, −20.23, −29.87 and −33.92 dB, respectively.

In Fig. 4(d), the amplitudes of the fundamental, second,

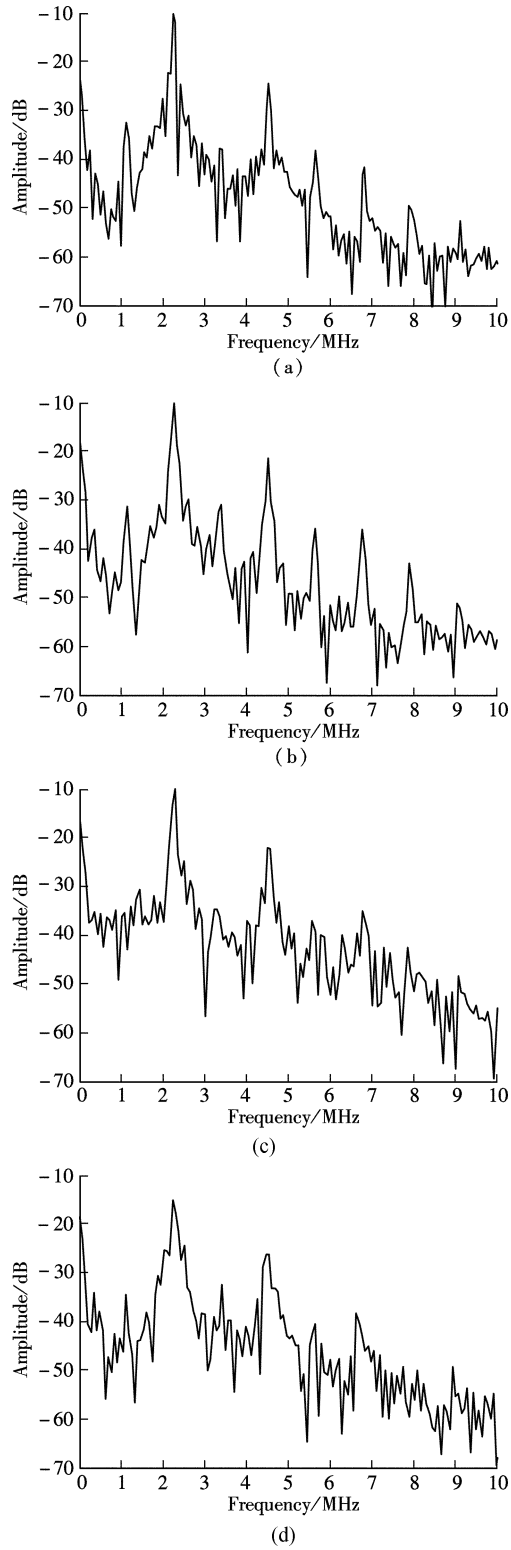

Fig. 4 Power spectrums of backscattered pressure from single microbubble. (a) G_s = 3.9 MPa, μ_s = 0.39 Pa · s; (b) G_s = 6.6 MPa, μ_s = 0.39 Pa · s; (c) G_s = 8.6 MPa, μ_s = 0.39 Pa · s; (d) G_s = 6.6 MPa, μ_s = 0.42 Pa · s

subharmonic and ultraharmonic components are −14.26, −24.86, −34.59 and −32.58 dB, respectively.

3 Conclusion

This paper theoretically simulates the oscillation of a single encapsulated microbubble and investigates the impacts of shear modulus and shear viscosity on the oscillation properties. First, setting a fixed value of the shear viscosity or the shear modulus and varying the other one to study the radii of microbubble oscillations, we find that the oscillation radii increase with the increase in the shear modulus while they decrease with the increase in shear viscosity. Using a similar method, a larger shear modulus causes larger amplitudes of the fundamental and harmonic components. At the same time, the smaller amplitudes of the fundamental and harmonic components can be obtained with a larger shear viscosity. Moreover, the shear modulus and shear viscosity affect subharmonic and ultraharmonic components much greater than the fundamental and second harmonic components. It is necessary to strictly control the value of shear viscosity and shear modulus . Secondly, we plot four power spectrums of backscattering at different shear moduli and shear viscosities: a shear viscosity of 0.39 Pa · s with a shear modulus of 3.9 MPa, 0.39 Pa · s with 6.6 MPa, 0.39 Pa · s with 8.6 MPa, 0.42 Pa · s with 6.6 MPa. These four power spectrums all show that the fundamental and harmonic components are significant but have different amplitudes and frequency bands. In summary, the studying of viscoelasticity of the shell provides a guidance for a prepared microbubble ultrasound contrast agent with suitable dynamic characteristics and excellent imaging ability.

References

[1] Goldberg B B, Liu J B, Forsberg F. Ultrasound contrast agents: a review [J]. *Ultrasound Med Biol*, 1994, **20**(4): 319 − 333.

[2] Forsberg F, Shi W T, Goldberg B B. Subharmonic imaging of contrast agents [J]. *Ultrasonics*, 2000, **38**(1/2/3/4/5/6/7/8): 93 − 98.

[3] Maikusa N, Fukami T, Yuasa T, et al. Fundamental study on subharmonic imaging by irradiation of amplitude-modulated ultrasound waves [J]. *J Acoust Soc Am*, 2007, **122**(1): 672 − 676.

[4] Cheung K, Couture O, Bevan P D, et al. In vitro characterization of the subharmonic ultrasound signal from definity microbubbles at high frequencies [J]. *Phys Med Biol*, 2008, **53**(5): 1209 − 1223.

[5] Patil A V, Reynolds P, Hossack J A. A nonlinear three-dimensional model for quantifying microbubble dynamics [J]. *J Acoust Soc Am*, 2010, **127**(2): 80 − 86.

[6] Shen C C, Yeh C K, Chen W S, et al. The effect of third harmonic transmit phasing on contrast agent responses for CTR improvement [J]. *Phys Med Biol*, 2008, **53**(21): 6179 − 6194.

[7] Basude R, Wheatley M A. Generation of ultraharmonics in surfactant based ultrasound contrast agents: use and advantages [J]. *Ultrasonics*, 2001, **39**(6): 437 − 444.

[8] Shi W T, Forsberg F. Ultrasound characterization of the nonlinear properties of contrast microbubbles [J]. *Ultrasound Med Biol*, 2000, **26**(1): 93 − 104.

[9] Postema M, Schmitz G. Ultrasonic bubbles in medicine: influence of the shell [J]. *Ultrasonics Sonochemistry*, 2007, **14**(4): 438 − 444.

[10] Yang F, Gu A Y, Chen Z P, et al. Multiple emulsion microbubbles for ultrasound imaging [J]. *Materials Letters*, 2008, **62**(1): 121 − 124.

[11] Church C C. The effects of an elastic solid surface layer on the radial pulsations of gas bubbles [J]. *J Acoust Soc Am*, 1995, **97**(3): 1510 − 1521.

[12] Hoff L, Sontum P C, Hovem J M. Oscillations of polymeric microbubbles: effect of the encapsulating shell [J]. *J Acoust Soc Am*, 2000, **107**(4): 2272 − 2280.

[13] Katiyar A, Sarkar K, Forsberg F. Modeling subharmonic response from contrast microbubbles as a function of ambient static pressure[J]. *J Acoust Soc Am*, 2011, **129**(4): 2325 − 2335.

膜壳黏弹性对单个微气泡非线性振动的影响

杨 莉 杨 芳 陈 平 顾 宁

(东南大学生物电子学国家重点实验室,南京 210096)
(东南大学江苏省生物材料与器件重点实验室,南京 210096)

摘要:基于 Church-Hoff 模型从理论上研究了具有有限厚度的单个包膜微气泡在超声辐射下的非线性振动情况. 分别研究了膜壳黏弹性对微气泡径向振动、基频成分和谐波成分的影响. 径向振动峰值、功率谱基波和谐波的幅值都随着膜壳剪切模量以 0.1 MPa 的间隔从 0 ~ 10 MPa 逐渐增大而增大,随着剪切黏性以 0.01 Pa · s 的间隔从 0 ~ 1 Pa · s 逐渐增大而减小. 次谐波和超谐波成分幅值波动范围大于基波和二次谐波成分,即微气泡膜壳黏弹性对次谐波和基波信号的影响大于对基波和二次谐波的成分影响. 这就使得调整微气泡膜壳黏弹性至合适的数值以制备得到具有较好的次谐波和超谐波成像的微气泡这一潜在方法成为可能. 最后,任选取基波和谐波成分都较为显著的 4 对黏弹性处以示说明,其剪切黏性和剪切模量分别为:0.39 Pa · s 和 3.9 MPa;0.39 Pa · s 和 6.6 MPa;0.39 Pa · s 和 8.6 MPa;0.42 Pa · s 和 6.6 MPa.

关键词: 微气泡; 黏弹性; 径向振动; 谐波成像
中图分类号: O422.7